CLM - P 457

CLM - P 457

UKAEA RESEARCH GROUP

Preprint

PLASMA DIAGNOSIS OF A HALL ACCELERATOR DISCHARGE

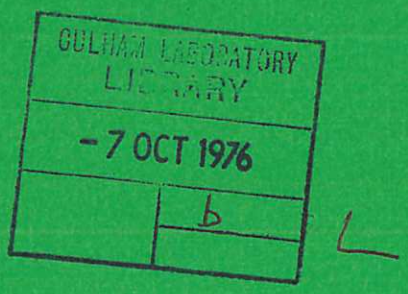

P J LOMAS

CULHAM LABORATORY
Abingdon Oxfordshire
1976

CLM-P 457

PLASMA DIAGNOSIS OF A HALL ACCELERATOR DISCHARGE

P.J. Lomas

Culham Laboratory, Abingdon, Oxon, OX14 3DB, UK
(Euratom/UKAEA Fusion Association)

and

Imperial College, London, S.W.7.

A B S T R A C T

The results of plasma measurements on a two stage, high current density ($\sim$ 50 A/cm^2) Hall accelerator hydrogen plasma are described. These measurements show that though $\omega\tau$ is large so that the electrons are collisionless, the observed electron conductivity is anomalously high. This arises because of the existence of a $\sim$ 5 Mhz fluctuation in which the associated azimuthal electric field drives collisionless electron drift currents. Momentum and total energy balances are investigated. These are consistent with a large wall loss of ions, expected since the instability dominated accelerating voltage gives a small ratio of ion Larmor radius to stage length. The electron energy balance is studied so that this might provide the basis for a stability analysis.

(Submitted for publication in Journal of Physics D).

March 1976

1. Introduction

Hall accelerators for fusion applications have been operated over a wide range of currents and voltages, from ~ few amps at ~ 20 kV to ~ 1 kA at ~ 1 kV, in single stage, two stage and multi-stage configurations (Morozov 1968, Cole 1970, Zubkov 1972, Cole 1974). However low fractions of ion current to discharge current and poor beam collimation lead to the conclusion (Sweetman 1971) that Hall accelerators are not competitive with conventional sources of fast ions, for the energies (10 keV to 40 keV) required for neutral injection experiments. Although there have been plasma measurements made on such devices, (Lary 1963, Zubkov 1971, Abramov 1974, Lomas 1974) these have been far from comprehensive, and it is not clear why the performance is so poor.

A slow mode of instability has been observed (Janes 1966) to manifest itself as a spoke-like streamer. This is important if the neutral density is high, and has been shown to be electrothermal in nature (Lomas 1975, 1976). However, this paper concerns a discharge at time ~ 500 μs, after this structure has disintegrated. Plasma diagnosis shows the electrons to be collisionless. The current conduction is discussed in this light, and the dominant plasma mechanisms examined.

2. The Plasma Conditions

Plasma measurements have been performed on a two stage, high current device similar to that described by Cole (1970), and which is illustrated in figure 1. A ~ 1 kA discharge across the radial magnetic field stages is formed by breakdown of a pulse of ~ 100 mtorr of hydrogen to give a reproducible current carrying streamer which

lasts for ~ 100 μs (Lomas 1974, 1975). After this time no such regular structure is observed, though fluctuations occur on a timescale of ~ 200 ns.

The ion current due to plasma acceleration is determined by a double plane probe biased to collect ions, but the variation of this current between anode and cathode in figure 2 contrasts results obtained in a low current density discharge (Zubkov 1971), where the ion current reaches a plateau of ~ $\frac{1}{3}$ of the discharge current by half-way along the first stage. In figure 2 there is also a plateau in the first stage, but the ion flux increases in the second stage until at the cathode the ions carry 350 ± 50 amp out of a total 1.0 kA discharge.

The electron temperature, estimated from the ion probe characteristic at zero bias voltage, allows the absolute and relative Balmer line intensities to be used to give both electron and neutral H atom densities when data from the collisional-radiative population model is employed (Johnson 1973, Bates 1962). Figure 3 shows these three quantities, n_e, N and T_e as functions of position from anode to cathode. Despite the poor sensitivity of the method, the atomic neutral density can be seen to fall by two orders of magnitude over the two stages, and this is due to charge-exchange with the ion flux and depletion of molecular neutrals by dissociative recombination. The degree of ionisation is still low, $\leqslant$ 1% because the electron density falls also.

Although the atomic ionisation rate is sensitively dependent upon n_e and T_e, this can be determined from the absolute intensity of Balmer α emission in a manner that is only weakly dependent upon n_e and T_e (Johnson 1973). The ionisation rate determined in this

way is shown in figure 4, where the two peaks correspond to the beginning of each stage. This is large at the anode since n_e and N are large, but the peak in the second stage is a consequence of the rise in T_e there.

To complete the picture, the axial electric field, measured with a single point probe, and the applied radial magnetic field are shown in figures 5 and 6.

3. The Value of $\omega\tau$

If the magnetic and electric fields are $\underline{B} = (B_r, 0, 0)$ and $\underline{E} = (0, 0, E_z)$ in a cylindrical system, then the generalised Ohm's Law gives the currents in the plane perpendicular to $\underline{B}$:-

$$J_z = \frac{\sigma}{1 + (\omega\tau)^2} E_z + neV_z$$

$$J_\theta = \frac{\sigma}{1 + (\omega\tau)^2} (V_z B - \omega\tau E_z) \qquad \ldots (1)$$

where pressure gradients and azimuthal motions have been neglected. The parameter $\omega\tau$, the product of electron gyrofrequency ω and electron collision time, τ, characterises the current flow. If $\omega\tau$ is large, the electron conduction current $J_{ze} = \sigma E_z / 1 + (\omega\tau)^2$ is small compared to the current $J_{zi} = neV_z$ due to accelerated ions, and the Hall current $J_\theta = - neE_z/B_r$ is due to electron $\underline{E} \wedge \underline{B}$ drifts. However if $\omega\tau$ is small, the electron conduction current approaches the magnetic field free value and will be larger than any ion current.

The value of $\omega\tau$ can be calculated for the plasma conditions of section 2, if account is taken of collisions with ions and neutrals, and is shown in figure 7. $\omega\tau$ is high, typically $\sim$ 100 in the first stage and $\sim$ 1000 in the second. That this does not give

the expected low values of axial electron conduction current can be seen by evaluating an effective $\omega\tau$, $\omega\tau_{eff} = \left(\frac{\sigma E_z}{J_{ze}} - 1 \right)^{\frac{1}{2}}$, using the calculated Spitzer conductivity (Spitzer 1955). This is also plotted in figure 7, revealing a discrepancy of two orders of magnitude, demonstrating that the cross-field electron conductivity is much larger than the collisional value. Notice that this value $\omega\tau_{eff}$ does not indicate an effective collision time since the true collision time has been used in its evaluation. Rather it indicates an effective magnetic field strength expressed in a dimensionless form.

Since the electrons are essentially collisionless, there will be an axial electron E/B drift current, $J_z = neE_\theta/B_r$, due to an observed fluctuating azimuthal electric field of magnitude $E_\theta \sim 2 \times 10^4$ V/M. This will account for the observed electron current if n_e and E_θ are in phase. Unfortunately measurement of the phase relationship is made difficult by the frequencies, ~ 5 Mc/s, though good correlation between n_e and E_θ fluctuations has been demonstrated for the correspondingly lower frequencies seen in a ~ 1 amp, single stage discharge in Argon (Morozov 1973).

4. The Particle Balance

The inflow of hydrogen molecules is $3 \pm 1. 10^{24}$ molecules $m^{-2} s^{-1}$ over the annular cross-section of the discharge chamber, whereas the flux of accelerated ions at the cathode is, by figure 2, $3 \pm 1. 10^{23}$ ions $m^{-2} s^{-1}$. The flux of hydrogen atoms obtained from a Balmer Doppler profile at the cathode is $3 \pm 2. 10^{24}$ atoms $m^{-2} s^{-1}$. Although the errors do not preclude a comparable flux of molecules, it can be seen that the gas efficiency is poor, typically only 10%.

5. The Momentum Balance

The measurement of ion flux and density allow estimates to be made of the spatially resolved mean ion energies as in figure 8,

assuming either H_2^+ or H^+ ions to dominate. Also shown is the energy of an ion freely accelerated from the anode. Close to the anode, where the ion mean free path for charge-exchange is only $\sim$ 1 mm, the low ion energies $\sim$ few eV are to be expected, but later in the first stage where mean free paths are $\sim$ 1 cm, the expected 50-100 eV ions are not seen. It is likely that this is a consequence of wall impact of ions due to Larmor radii being $\sim$ stage length (Lomas 1975), which would account for the plateau in ion flux over this stage. In the second stage, ions have energies comparable to that acquired by free acceleration in the electric field from the region 6 to 8 cm from the anode, i.e. from the region of peaked ionisation at the beginning of the second stage, and most of these ions escape the cathode aperture.

The neutral atom and ion momentum flux densities in the second stage, are respectively 900 and 800 kg $m^{-1}s^{-2}$ to within a factor of 2, the latter assuming the ions to be H^+. By comparison Hall current momentum input is 2500 ± 500 kg $m^{-1}s^{-2}$. so that, though these balance, the errors are too large to reveal contributions from either wall impact of ions or molecular neutrals.

6. The Electron Energy Balance

The terms in an electron energy balance of the form:-

$$\frac{J^2}{\sigma} = \frac{3\ nkT_e}{\tau_{en}} \frac{m_e}{m_n} + H + n\ NS\ eE_I + \frac{2.5\ nk^2T^2}{m_e\ \nu\ L_r^2}$$

have been examined, where the symbols have their usual meaning. The first term on the right represents electron cooling due to collisions with cold neutrals. The result of collisions with ions is heating by a Spitzer (1955) equipartion between electrons at

temperature T_e and ions of mean energy W eV, $H = 10^{-35} (W - T_e) n_e^2$ watts/M^3. The ionisation energy uses the results of figure 4, where the ionisation potential is E_I = 13.6 eV. Thermal conduction loss to the walls is characterised by a radial temperature scale length L_r = 1 cm, half the channel width. In the second stage where the electron mean free path $\lambda_{ie} \gtrsim L_r$, this is flux limited. These terms are tabulated in columns 2 to 9 of table 1 for various distances from the anode.

Note that there is a discrepancy between the ohmic heating estimated from J^2/σ and $J_{ze}E_z$ which should be equivalent since $\omega\tau$ is large. This is not wholly unexpected since figure 7 has already demonstrated that $J_{ze} = \sigma E_z/(1 + (\omega\tau)^2)$ does not hold. Since current is expected to flow in the high conductivity regions, the estimate of J^2/σ is unlikely to be affected significantly by fluctuations. In the absence of fluctuations, the difference $J_{ze}E_z - J^2/\sigma$ represents the input to directed electron energy. This suggests that large powers 100-1000 kW (depending upon the correlation between J_{ez} and E_z) will be deposited on the anode.

In the first stage the losses due to ionisation, conduction and neutral collisions balance the ohmic heating due to the axial electron current. In the second stage, ohmic heating by the Hall currents is balanced by flux limited thermal conduction. The higher electron temperature in the second stage is a consequence of the improved thermal isolation brought about by flux limited conduction.

7. The Total Energy Balance

Using an analysis similar to the proceeding sections, the total energy balance of table 2 has been compiled. The lower limit on energy deposited on the anode is estimated from the surface melting time (Lochte-

Holtgreven, 1968). Although balance is obtained, this is not sufficiently accurate to demonstrate energy loss due to wall impact of ions, though this may be as large as 50% of the energy input. The ratio of total output power in ions and neutrals to total input power confirms Cole's calorimetric estimate of 60% (Sweetman, 1971, Cole 1971). A large fraction of the output power appears in the neutrals, and this could be of interest for neutral injection experiments.

8. Conclusions

Measurements of plasma conditions for a 1 kA Hall accelerator discharge in hydrogen after the disappearance of spoke structure reveal that, though $\omega\tau$ is large, i.e. the electrons are collisionless, the discharge current is still carried predominantly by electrons in contradiction of the simple theory. The current conduction is in fact dominated by fluctuating azimuthal electric fields. Low ion energies attributable to wall impact are deduced for the first stage. Second stage ions are freely accelerated out of the device to give the characteristic highly divergent beam.

The electron energy balance is dominated by ohmic heating, thermal conduction loss and ionisation. However, in the second stage, the long electron mean freee path limits the conduction loss so that overall the electrons only appear to contribute a small fraction to the total energy balance. A large fraction of the energy appears in the neutrals. A large energy loss due to ion-wall inpact is not inconsistent with the observations.

The results and discussion here presented allow stability to be examined (Lomas 1975) and this will be reported elsewhere.

Acknowledgements

This work was carried out at Culham whilst the author was on attachment from Imperial College, London. Thanks are warmly extended to Dr H.C. Cole of Culham Laboratory and Dr J.D. Kilkenny of Imperial College for many discussions.

I gratefully acknowledge the receipt of a studentship from the S.R.C. during the major part of this work.

References

Abramov V A, Zubkov I P and Kislov A Ya 1974, Sov. Phys. Tech. Phys. 18 1609.

Bates D R, Kingston A E and McWhirter R W P 1962, Proc. Roy. Soc. A267 155.

Cole H C 1970, Nuclear Fusion 10 271.

Cole H C 1971, Unpublished results.

Cole H C, Saunders B D, Naylor G O R and Terry M J 1974, 2nd Symposium on Ion Sources and Formation of Ion Beams, Berkeley.

Janes G S and Lowder R S 1966, Phys. Fluids 9 115.

Johnson L C and Hinnov E 1973, J. Quant. Spectrosc. Radiat. Trans. 13 333.

Lary E C, Meyerand R G and Salz F 1963, VI Ionisation Phenomena in Gases, Paris.

Lochte-Holtgreven (ed) 1968, "Plasma Diagnostics". North Holland.

Lomas P J and Kilkenny J D 1974, 1st Annual Plasma Conf. Institute of Physics, Bangor.

Lomas P J and Kilkenny J D 1975, Proc. VIII European Fusion Conf. Lausanne.

Lomas P J 1975, Ph.D. Thesis, London University.

Lomas P J and Kilkenny J D. 1976. To be published.

Morozov A I, Kislov A Ya and Zubkov I P 1968, Zh. E.T.F. Pis'ma 7 224.

Morozov A I, Esipchuk Yu V, Tilinin G N, Trofimov A V, Sharov Yu A, Shchepkin G Ya 1972, Sov. Phys. Tech. Phys. 17 38.

Morozov A I, Esipchuk Yu V, Kapulkin A M, Nevrovskii V A and Smirnov V A 1973, Sov. Phys. Tech. Phys. 18 615.

Spitzer L 1955, Physics of Fully Ionised Gases, Wiley.

Sweetman D R 1971, IAEA Paper No CN 28/K-5 Madison.

Zubkov I P, Kislov A Ya and Morozov A I 1971, Sov. Phys. Tech. Phys. 16 695.

Zubkov I P, Kislov A Ya and Morozov A I 1972, Sov. Phys. Tech. Phys. 17 712.

Z (cm)	j_{ez}^2/σ Watt / m^3	$j_{\theta e}^2/\sigma$ Watt / m^3	$j_{ez} E_z$ Watt / m^3	Thermal Conduction loss. W/m^3	Ionization Energy W/m^3	Neutral Cooling W/m^3	Ion Heating W/m^3	Flux Limited Conduction Loss. W/m^3	Wall Dominated Ohmic input. W/m^3
2	4.5×10^7	$\leqslant 4\times10^5$	1.4×10^9	3×10^6	4×10^6	2×10^6	$\leqslant 10^3$	-	-
4	1.7×10^7	$\leqslant 4\times10^5$	5.4×10^8	2×10^7	1×10^6	7×10^4	$\leqslant 10^3$	-	-
6	5.1×10^6	$\leqslant 4\times10^5$	1.1×10^9	6×10^8	2×10^7	5×10^4	$\leqslant 10^3$	2×10^8	6×10^7
8	6.4×10^6	2×10^7	2.4×10^9	8×10^8	8×10^6	1×10^4	6×10^3	8×10^7	2×10^8
10	6.1×10^6	2×10^7	2.2×10^9	7×10^8	4×10^6	5×10^3	3×10^4	5×10^7	3×10^8
12	5.6×10^6	2×10^7	2.0×10^9	2×10^8	2×10^6	2×10^3	2×10^4	1×10^7	4×10^8
Accuracy	50%	50%	~ 20%	factor ~ 2	factor ~ 2	factor ~ 4	factor ~ 4	factor ~ 3	factor ~ 2

Table 1

The electron energy balance. Columns 2-8 compare energy input and loss estimated on a basis of electron-ion and electron-neutral collisions. Column 9 gives the flux limited thermal conduction loss for the second stage where $\lambda_{ie} \geqslant L$. Column 10 gives the 'worst' estimate of the contribution of wall collisions to the Ohmic heating.

TABLE 2. THE TOTAL ENERGY BALANCE

Item	Power kW	Accuracy
Total power input	1500	15%
Ion beam power output	300	10%
Neutral beam power output	400	factor 2
Electron ionisation and conduction loss	40	factor 2
Power into anode	$\geq$ 100	factor 2

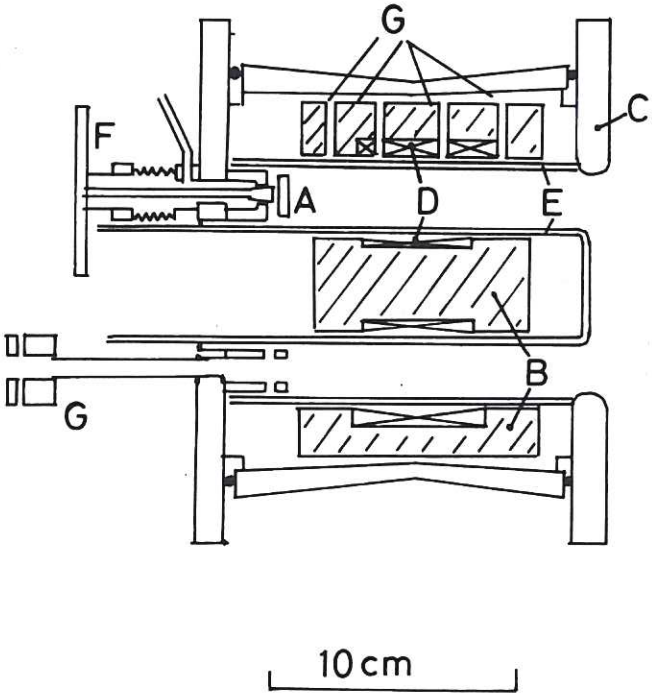

Fig.1 The two stage Hall Accelerator showing A anode, B iron magnets, C cathode, D coils, E wall, F gas valve, G ports.

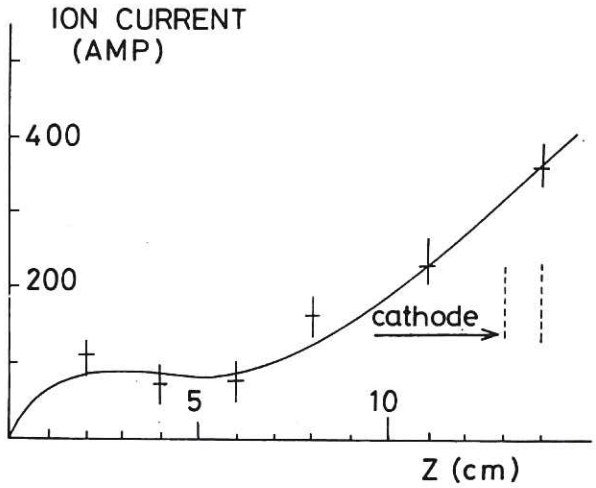

Fig.2 The axial variation of the total current carried by the ions at time 500 μs after initiation of the discharge.

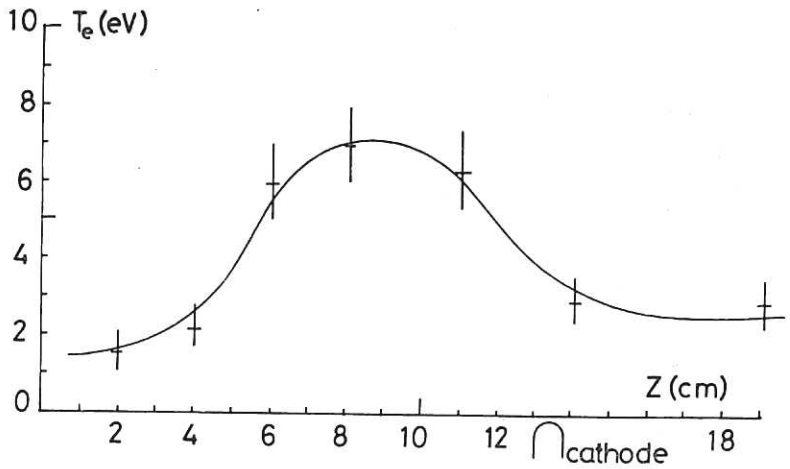

Fig.3a The axial dependence of electron temperature T_e.

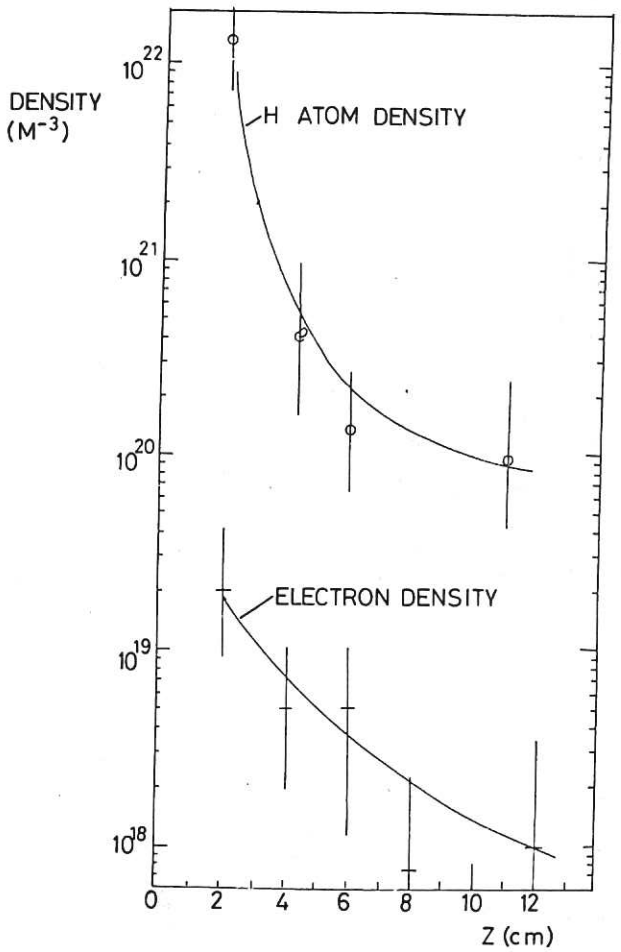

Fig.3b The axial dependence of electron and neutral densities n_e and $N(m^{-3})$.

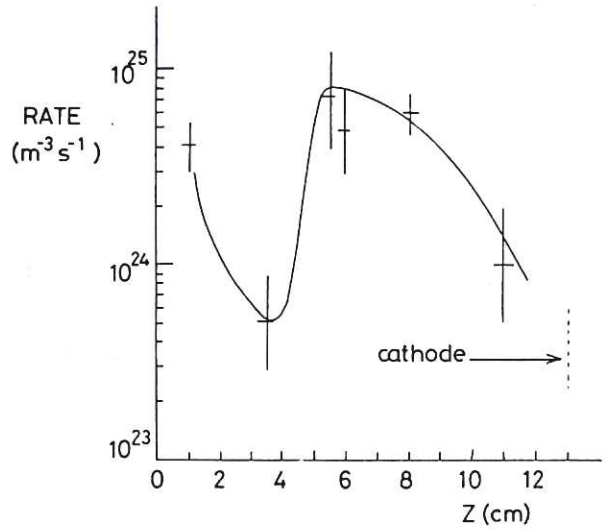

Fig.4 The ionisation rate between anode and cathode at 500 μs.

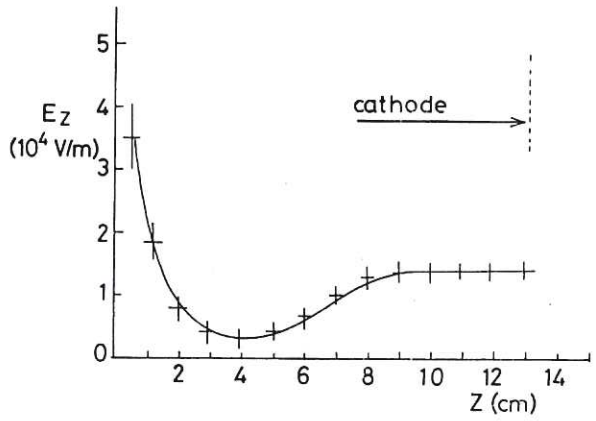

Fig.5 The axial electric field at 500 μs between anode and cathode.

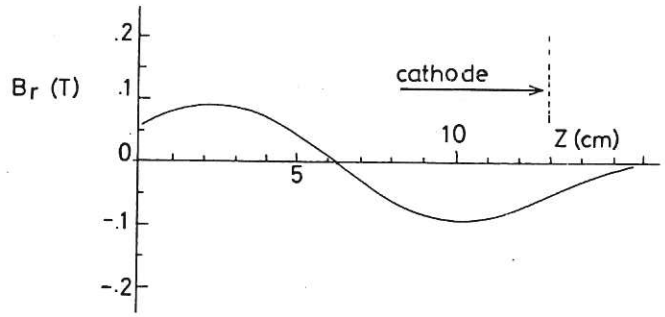

Fig.6 The applied radial magnetic field.

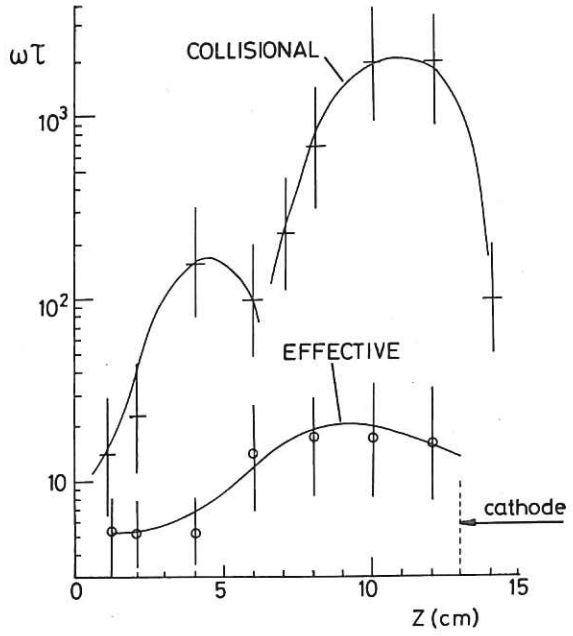

Fig.7 The value of $\omega\tau$ at time 500 μs calculated from graphs 3. Also shown is the "effective' $\omega\tau$ determined from the observed cross-field electron conductivity.

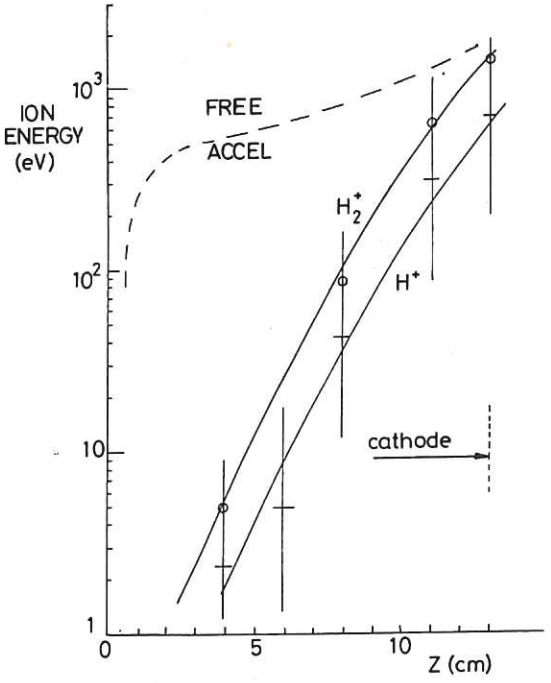

Fig.8 The mean ion energy calculated from the ion current and n_e assuming either H^+ or H_2^+ ions dominant. Also shown dotted is the energy of a single charge freely accelerated from the anode in the electric field of Fig.5.